Meshless analysis of nonlocal boundary value problems in anisotropic and inhomogeneous media

Zaheer-ud-Din[a,b*], Muhammad Ahsan[b,c], Masood Ahmad[b], Wajid Khan[b], Emad E. Mahmood[d,e], Abdel-Haleem Abdel-Aty[f,g]

[a]Department of Basic Sciences, CECOS University of IT and Emerging Sciences Peshawar, Pakistan.

[b]Department of Basic Sciences, University of Engineering and Technology Peshawar, Pakistan.

[c]Department of Mathematics, University of Sawabi, Pakistan.

[d]Department of Mathematics, College of Science, Taif University, Saudi Arabia.

[e]Department of Mathematics, Faculty of Science, Sohag University, Egypt.

[f]Department of Physics, College of Sciences, Unversity of Bisha, Saudi Arabia.

[g]Physics Department, Faculty of Al-Azhar University, Egypt.

Abstract

In this work, meshless methods are applied for the solution of two-dimensional steady-state heat conduction problems with nonlocal multi-point boundary conditions (NMBC). These meshless procedures are based on multiquadric radial basis function (MQ RBF) and its modified version (i.e. integrated MQ RBF). The proposed meshless methods which were recently published in [1] is compared with standard collocation method (i.e. Kansa's method). Three different sorts of solution domain are considered in which Dirichlet boundary condition is specified on some part of the boundary and is related to the unknown function values at a discrete set of interior points. The influence of NMBC on the accuracy and condition number of the system matrix associated to the proposed methods is investigated. The sensitivity of the shape parameter is also analyzed in the proposed methods. Performance of the proposed approaches in terms of accuracy and efficiency is confirmed on the benchmark problems.

Keywords: Meshless method; Integrated MQ RBF; Steady-state heat conduction equation.

1 Introduction

Meshless methods for the solution of differential equations are being successfully applied in various fields of science and engineering, and, they are more effective and suitable for complex domains as compared to mesh-based numerical methods. Since a set of independent points are required for meshless methods, so they are often better suited for complex geometries to cope with. The computational costs associated with mesh-based numerical methods are hence eliminated. Because of mesh generation, mesh-based methods are time-consuming [2]. Meshless methods can be easily extended to multi-dimensional complex geometries. In comparison to meshless methods, other traditional numerical methods such as finite difference methods, finite element methods, or finite volume methods are usually limited to problems involving two or three spacial variables (space dimensions).

Literature suggests that MQ RBF is considered the best in accuracy among different types of RBFs, however, the shape of the function is controlled by shape parameter ϵ. The ϵ effects the accuracy of the method where its optimal value can lead to good approximations. However,

*The author to whom all the correspondence should be addressed. Email:zaheeruddin@cecos.edu.pk (Zaheer-ud-Din)

Preprints (www.preprints.org) | NOT PEER-REVIEWED | Posted: 30 September 2020 doi:10.20944/preprints202009.0751.v1

determination of the optimal value of the ϵ is an open problem and there is no such mathematical theory developed so far that find its optimal value. Another drawback is the condition number of the interpolation matrix. The ill-conditional system matrix arises in the case of globally supported RBFs as the separation distance $\frac{1}{2}\max_{i\neq j}\|x_i - x_j\|_2$, $i, j = 1, 2, 3, ..., N$, between data points decreases for fixed values of the shape parameter ϵ [3]. Many prominent researchers have used a different value of the shape parameter in the hope to accurately handle such problems. Both constant and variable shape parameters are recommended. For instance, in an early work, a formula which depends on the spacing between centers for shape parameter was given by Hardy [4]

$$\epsilon = \frac{0.815\sum_{j=1}^{N} d_j}{N},$$

where N is number of collocation points and d_j is the distance from the j^{th} center to its nearest neighbor. Later on, a smallest circle enclosing all data points is considered and the shape parameter was recommended as $\frac{1.25}{\sqrt{N}}$ times diameter of this circle [5]. The shape parameter $\frac{2}{\sqrt{N}}$ was used for solution of nonlinear PDEs in [6]. In [7], two optimal values of the shape parameter 1.03 and 1.42 were recommended for MQ RBF whereas for Gaussian basis, a range $0.003 - 0.03$ was given, for solving cantilever beam and perforated strip plate problems. In [8–10], it is concluded that splitting of shape parameter into x- and y- axes give good result i.e., $\epsilon_x = h_x N_x^2$ and $\epsilon_y = h_y N_y^2$, where h_x and h_y are positive constants, but condition number of the collocation matrix is high. Further different selection procedures of shape parameter can be found in [11–19].

In this paper, a meshless discretization technique based on MQ RBF and its modified form i.e integrated MQ RBF is applied for the numerical solution of elliptic PDEs with nonlocal boundary conditions (NBC). In the last decades, RBF-based collocation technique for the solution of nonlocal boundary value problems has been vital research area in many branches of science and hence was successfully applied to solve such problems numerically [20–22]. One-dimensional hyperbolic equation with integral boundary condition was studied in [23]. The two-dimensional diffusion equation subject to a nonlocal condition involving double integral along with Neumann's boundary conditions was formulated in a rectangular region. Such type of problem is solved numerically using meshless collocation method [24]. In paper [25], The RBF-based collocation technique was also applied to investigate the influence of nonlocal conditions on the optimal selection of shape parameter ϵ, conditioning, and accuracy of the method. A nonlocal two-dimensional Poisson equation was solved with two-point and integral boundary condition which was formulated on one side of the rectangular region. Later, in [10], comparison of RBF-based collocation technique with Haar wavelets-based collocation technique was studied for the same problem. Because of the splitting of shape parameter into x- and y-direction its effect on the accuracy of the problem in hand was also investigated. The influence of shape parameter ϵ and the distribution of nodes on the accuracy of the RBF-based collocation technique was investigated by considering multidimensional linear elliptic equation with integral conditions [26]. Recently, the RBF-based meshless method has been applied to elliptic PDEs with NMBC [27].

Since it is known that meshless method can be successfully applied to solve such kind of nonlocal problems. However, it was shown (e.g., see paper [10, 25, 27]) that due to the nonlocal parameter γ, the condition number κ of the system matrix involved and accuracy of the method is affected. It is shown that RBF-based collocation technique give quite good results for the optimal value of shape parameter [25, 27]. On the other hand, for the optimal value of shape parameter, the accuracy and conditioning are also slightly affected by the NBC. The aim of this paper is to investigate the effect of this parameter on the property of the RBF-based method using integrated MQ RBF. Now-a-days, integrated RBF(s) are successfully implemented in solving miscellaneous

Preprints (www.preprints.org) | NOT PEER-REVIEWED | Posted: 30 September 2020 doi:10.20944/preprints202009.0751.v1

differential equations. An MQ-RBF integrated twicely with fixed value of shape parameter ϵ is used by [28] to solve one-dimensional problems. Elliptic problems are solved by [29] through multi domain integrated RBF collocation method. Higher order ODEs and PDEs are solved by integrated RBF method in the papers [30, 31]. Further detail about integrated RBFs can be found in [3, 32–34].

2 Governing equation

A general form of the diffusion equation is given by [1]

$$k_{1,1}(\hat{\mathbf{v}})\frac{\partial^2}{\partial x^2}u(\hat{\mathbf{v}}) + 2k_{1,2}(\hat{\mathbf{v}})\frac{\partial^2}{\partial x\partial y}u(\hat{\mathbf{v}}) + k_{2,2}(\hat{\mathbf{v}})\frac{\partial^2}{\partial y^2}u(\hat{\mathbf{v}}) + \left(\frac{\partial}{\partial x}k_{1,1}(\hat{\mathbf{v}}) + \frac{\partial}{\partial y}k_{1,2}(\hat{\mathbf{v}})\right)\frac{\partial}{\partial x}u(\hat{\mathbf{v}}) + \left(\frac{\partial}{\partial x}k_{1,2}(\hat{\mathbf{v}}) + \frac{\partial}{\partial y}k_{2,2}(\hat{\mathbf{v}})\right)\frac{\partial}{\partial y}u(\hat{\mathbf{v}}) = f(\hat{\mathbf{v}}), \qquad \hat{\mathbf{v}} = (x, y) \in \Omega. \tag{1}$$

The above model is subject to mixed boundary conditions:
• Classical Dirichlet boundary conditions:

$$u(\hat{\mathbf{v}}) = g(\hat{\mathbf{v}}), \qquad \hat{\mathbf{v}} \in \Gamma_1. \tag{2}$$

• Nonlocal multipoint boundary conditions:

$$u(\hat{\mathbf{v}}) - \sum_{l=1}^{n} \gamma u(\hat{\mathbf{v}}_l^\star) = h(\hat{\mathbf{v}}), \qquad \hat{\mathbf{v}} \in \Gamma_2, \quad \hat{\mathbf{v}}^\star \in \Omega^\star, \tag{3}$$

where $\Omega^\star \subset \Omega$ are set of discrete distinct scattered points inside the solution domain and n is the number of these scattered points. Throughout the paper we will take $n = 10$ otherwise it will be mentioned. It is also assumed that the distribution of the points $\hat{\mathbf{v}}_l^\star$ on the solution domain will be fixed. The given functions are $k_{1,1}$, $k_{1,2}$, $k_{2,2}$, f, g, h, and the parameter γ. Ω is the interior portion of the solution domain and $\Gamma = \Gamma_1 \cup \Gamma_2$ are the boundary part of the solution domain such that $\Gamma_1 \cap \Gamma_2 = \emptyset$ and $\Gamma_2 \neq \emptyset$. The NBC defined on the boundary Γ_2 is reduced to Dirichlet boundary condition when $\gamma = 0$.

3 The numerical scheme

Let us divide the solution domain into three disjoint set. The set of inner distinct scattered nodes

$$\hat{\Omega} = \{(x_j, y_j)\}_{j=1}^{N}, \tag{4}$$

and the set of distinct scattered boundary points

$$\hat{\Gamma}_1 = \{(x_{l_1}, y_{l_1})\}_{l_1=1}^{M_1}, \tag{5}$$

$$\hat{\Gamma}_2 = \{(x_{l_2}, y_{l_2})\}_{l_2=1}^{M_2}, \tag{6}$$

such that $\hat{\Omega} \subset \Omega$, $\hat{\Gamma}_1 \subset \Gamma_1$, and $\hat{\Gamma}_2 \subset \Gamma_2$. N is the total number of data points inside the solution domain and $M = M_1 + M_2$ is the total number of boundary points on the boundary Γ. We

Preprints (www.preprints.org) | NOT PEER-REVIEWED | Posted: 30 September 2020 doi:10.20944/preprints202009.0751.v1

also assume that the points $\hat{\mathbf{v}}^\star$ are not included in $\hat{\Omega}$ i.e., $\Omega^\star \subset \Omega$ but $\Omega^\star \nsubseteq \hat{\Omega}$. Furthermore, throughout the paper a given RBF inside the solution domain is denoted by

$$\phi_i(\hat{\mathbf{v}}) = \phi(\|\hat{\mathbf{v}} - \hat{\mathbf{v}}_i\|_2), \tag{7}$$

where the centers $\hat{\mathbf{v}}_i = (x_i, y_i)$, $i = 1, 2, ..., N$ are distributed inside the solution domain. Similarly, if the centers $\hat{\mathbf{v}}_k = (x_k, y_k)$, $k = 1, 2, ..., M$ are distributed on the boundary Γ, then the RBF on the boundary is given by

$$\phi_k(\hat{\mathbf{v}}) = \phi(\|\hat{\mathbf{v}} - \hat{\mathbf{v}}_k\|_2). \tag{8}$$

Recently, RBF-based method is used to solve two-dimensional steady-state PDEs with three different types of boundary conditions (Dirichlet, Neumann, and Robin boundary conditions) in anisotropic and inhomogeneous media [1]. In [1], an approximate solution is sought in the form

$$u(\hat{\mathbf{v}}) = u_g(\hat{\mathbf{v}}) + \sum_{i=1}^{N} \lambda_i \psi_i(\hat{\mathbf{v}}), \tag{9}$$

where basis $u_g(\hat{\mathbf{v}})$ is a smooth function which satisfy the boundary conditions, $\psi_i(\hat{\mathbf{v}})$ is a sum of the given RBF. $\omega_i(\hat{\mathbf{v}})$ called the correcting function, is chosen such that:

$$\phi_i(x_k, y_k) + \omega_i(x_k, y_k) = 0. \tag{10}$$

It is to be noted that in paper [1], trigonometric basis, polynomial basis and RBF basis are used to find the functions $u_g(\hat{\mathbf{v}})$ and the correcting function $\omega_i(\hat{\mathbf{v}})$. However, we use here just MQ RBF and integrated MQ RBF to find these functions.

This algorithm strictly divide the approximation of boundary conditions and approximation of differential equation inside the solution domain in case of Dirichlet, Neumann, and Robin boundary conditions (for more detail see [1]). However, in case of NBC the values of the solution u on the boundary part Γ_2 is related to the values at the interior points. So, boundary conditions cannot be approximated separately because the values of the solution u at the boundary Γ_2 are unknown.

Equation (9) can be rewritten in the form

$$u(\hat{\mathbf{v}}) = \sum_{k=1}^{M} \beta_k \phi_k(\hat{\mathbf{v}}) + \sum_{i=1}^{N} \lambda_i (\phi_i(\hat{\mathbf{v}}) + \omega_i(\hat{\mathbf{v}})), \tag{11}$$

where

$$\omega_i(\hat{\mathbf{v}}) = \sum_{k=1}^{M} P_{k,i} \phi_k(\hat{\mathbf{v}}).$$

The correcting function $\omega_i(\hat{\mathbf{v}})$ are determined from condition (10). While, the unknown parameters β_k, $k = 1, 2, 3, ..., M$ and λ_i, $i = 1, 2, 3, ..., N$ are determined by substituting (11) in the governing equation (1) and collocate at the interior and boundary points of the solution domain.

Preprints (www.preprints.org) | NOT PEER-REVIEWED | Posted: 30 September 2020 doi:10.20944/preprints202009.0751.v1

i.e.,

$$\begin{aligned}
&\sum_{k=1}^{M}\beta_k\{k_{1,1}(\hat{\mathbf{v}})\frac{\partial^2}{\partial x^2}\phi_k(\hat{\mathbf{v}})+2k_{1,2}(\hat{\mathbf{v}})\frac{\partial^2}{\partial x\partial y}\phi_k(\hat{\mathbf{v}})+k_{2,2}(\hat{\mathbf{v}})\frac{\partial^2}{\partial y^2}\phi_k(\hat{\mathbf{v}})+\left(\frac{\partial}{\partial x}k_{1,1}(\hat{\mathbf{v}})+\frac{\partial}{\partial y}k_{1,2}(\hat{\mathbf{v}})\right)\frac{\partial}{\partial x}\phi_k(\hat{\mathbf{v}})+\\
&\left(\frac{\partial}{\partial x}k_{1,2}(\hat{\mathbf{v}})+\frac{\partial}{\partial y}k_{2,2}(\hat{\mathbf{v}})\right)\frac{\partial}{\partial y}\phi_k(\hat{\mathbf{v}})\}+\sum_{i=1}^{N}\lambda_i\{k_{1,1}(\hat{\mathbf{v}})\frac{\partial^2}{\partial x^2}(\phi_i(\hat{\mathbf{v}})+\omega_i(\hat{\mathbf{v}}))+2k_{1,2}(\hat{\mathbf{v}})\frac{\partial^2}{\partial x\partial y}(\phi_i(\hat{\mathbf{v}})+\omega_i(\hat{\mathbf{v}}))+\\
&\left(\frac{\partial}{\partial x}k_{1,1}(\hat{\mathbf{v}})+\frac{\partial}{\partial y}k_{1,2}(\hat{\mathbf{v}})\right)\frac{\partial}{\partial x}(\phi_i(\hat{\mathbf{v}})+\omega_i(\hat{\mathbf{v}}))+\left(\frac{\partial}{\partial x}k_{1,2}(\hat{\mathbf{v}})+\frac{\partial}{\partial y}k_{2,2}(\hat{\mathbf{v}})\right)\frac{\partial}{\partial y}(\phi_i(\hat{\mathbf{v}})+\omega_i(\hat{\mathbf{v}}))+\\
&k_{2,2}(\hat{\mathbf{v}})\frac{\partial^2}{\partial y^2}(\phi_i(\hat{\mathbf{v}})+\omega_i(\hat{\mathbf{v}}))\}=f(\hat{\mathbf{v}}), \qquad \hat{\mathbf{v}}\in\hat{\Omega},\\
&\sum_{k=1}^{M}\beta_k\phi_k(\hat{\mathbf{v}})=g(\hat{\mathbf{v}}), \qquad \hat{\mathbf{v}}\in\hat{\Gamma}_1,\\
&\sum_{k=1}^{M}\beta_k\left(\phi_k(\hat{\mathbf{v}})-\sum_{l=1}^{n}\gamma\phi_k(\hat{\mathbf{v}}_l^{\star})\right)-\sum_{i=1}^{N}\lambda_i\left(\sum_{l=1}^{n}\gamma\phi_i(\hat{\mathbf{v}}_l^{\star})\right)=h(\hat{\mathbf{v}}), \qquad \hat{\mathbf{v}}\in\hat{\Gamma}_2.
\end{aligned} \tag{12}$$

The above system (12) are solved for the unknowns β_k, $k=1,2,3,...,M$ and λ_i, $i=1,2,3,...,N$. The approximate solution u is obtained by substituting these unknowns in (11). The numerical implementation of this method contains two stages. At first stage, the correcting function $\omega_i(\hat{\mathbf{v}})$ is approximated. At the second stage, the correcting function $\omega_i(\hat{\mathbf{v}})$ is used to solve system (12). When $\phi(\hat{\mathbf{v}})$ is MQ RBF we named the method as RCM1 and when it is integrated MQ RBF the method is named as IRCM1.

The standard collocation method known as Kansa's approach is explained here. In Kansa's approach, the approximate solution is sought in the form

$$u(\hat{\mathbf{v}})=\sum_{i=1}^{N+M}\lambda_i\phi_i(\hat{\mathbf{v}}), \tag{13}$$

where the centers are distributed inside the solution domain and on the boundary i.e., $\hat{\mathbf{v}}_i\in\hat{\Omega}\cup\hat{\Gamma}_1\cup\hat{\Gamma}_2$. Substituting (13) in (1), (2) and, (3) we have

$$\begin{aligned}
&\sum_{i=1}^{N+M}\lambda_i\{k_{1,1}(\hat{\mathbf{v}})\frac{\partial^2}{\partial x^2}\phi_i(\hat{\mathbf{v}})+2k_{1,2}(\hat{\mathbf{v}})\frac{\partial^2}{\partial x\partial y}\phi_i(\hat{\mathbf{v}})+k_{2,2}(\hat{\mathbf{v}})\frac{\partial^2}{\partial y^2}(\phi_i\hat{\mathbf{v}})+\left(\frac{\partial}{\partial x}k_{1,1}(\hat{\mathbf{v}})+\frac{\partial}{\partial y}k_{1,2}(\hat{\mathbf{v}})\right)\frac{\partial}{\partial x}\phi_i(\hat{\mathbf{v}})+\\
&\left(\frac{\partial}{\partial x}k_{1,2}(\hat{\mathbf{v}})+\frac{\partial}{\partial y}k_{2,2}(\hat{\mathbf{v}})\right)\frac{\partial}{\partial y}\phi_i(\hat{\mathbf{v}})\}=f(\hat{\mathbf{v}}), \qquad \hat{\mathbf{v}}\in\hat{\Omega},\\
&\sum_{i=1}^{N+M}\lambda_i\phi_i(\hat{\mathbf{v}})=g(\hat{\mathbf{v}}), \qquad \hat{\mathbf{v}}\in\hat{\Gamma}_1,\\
&\sum_{i=1}^{N+M}\lambda_i\left(\phi_i(\hat{\mathbf{v}})-\sum_{l=1}^{n}\gamma\phi_i(\hat{\mathbf{v}}_l^{\star})\right)=h(\hat{\mathbf{v}}), \qquad \hat{\mathbf{v}}\in\hat{\Gamma}_2.
\end{aligned} \tag{14}$$

This system (14) of linear equations is solved for λ_i, $(i=1,2,3,...,N+M)$ to get the approximate solution (13) of (1). In this procedure when $\phi(\hat{\mathbf{v}})$ is MQ RBF, the method named as RCM2 and when it is integrated MQ RBF the method is named as IRCM2.

Preprints (www.preprints.org) | NOT PEER-REVIEWED | Posted: 30 September 2020 doi:10.20944/preprints202009.0751.v1

3.1 Integrated MQ RBF

It is shown in the numerical section that integrated RBF methods give quite a good result as compared to standard non-integrated RBF methods. In order to achieve new basis for numerical solution of differential equations, RBF is integrated several times w.r.t r. In the present paper, we will use MQ RBF as

$$\text{MQ} = \sqrt{1 + (\epsilon_o r)^2}, \tag{15}$$

where r is the Euclidean norm.

Six times integration of MQ RBF (15) with respect to r, give the basis functions [3]

$$\text{IMQ6} = \frac{\sqrt{1+(\epsilon r)^2}\left\{40(\epsilon r)^6 - 1518(\epsilon r)^4 + 1779(\epsilon r)^2 - 128\right\} + 105\epsilon r \sinh^{-1}(\epsilon r)\left\{8(\epsilon r)^4 - 20(\epsilon r)^2 + 5\right\}}{201600\epsilon^6}. \tag{16}$$

The parameter ϵ_o in (15) is a shape parameter but the symbol is changed to distinguish it from the shape parameter in (16). In our study ϵ_o will be represented the shape parameter for MQ and ϵ will be denoted the shape parameter for IMQ6. The MQ RBF can be integrated easily using a computer algebra system. In paper [3], the first four members of the integrated RBF family based on MQ RBF were listed. The benefit of IMQ6 is that it is not much sensitive to the shape parameter as compared to MQ. The IMQ6 basis function gives quite good results for a wide range of ϵ, but to find optimal ϵ is still challenge in this case as well. In case of IMQ6 basis, the value of ϵ is taken $\epsilon = 80$ in our study. But this value is not the optimal value of the shape parameter. In the case of MQ basis, we will take the value of $\epsilon_o = 2$ otherwise will be mentioned during the investigation.

4 Numerical experiments

In this section, the numerical results and the effect of non-local boundary condition (3) are demonstrated for (1). We discussed here different type of RBF-based collocation methods i.e., RCM1, IRCM1, RCM2, and IRCM2. The effect of the shape parameters on the accuracy and κ of the system matrices of the proposed methods is also investigated. This section shows that the proposed methods IRCM1 and IRCM2 are less sensitive to the selection of shape parameters as compared to RCM1 and RCM2.

Various error measures are used to estimate the accuracy of the numerical method. Among them one is L_{rms} error norm which is defined as

$$L_{rms} = \sqrt{\frac{1}{N}\sum_{i=1}^{N}[\mathbf{u}(\hat{\mathbf{v}}) - u(\hat{\mathbf{v}})]^2}, \tag{17}$$

where $\mathbf{u}(\hat{\mathbf{v}})$ and $u(\hat{\mathbf{v}})$ represent the exact and the approximate solutions respectively. One can also check the numerical stability of the method by κ of the system matrix involved. A well conditioned system matrix is having small value of κ, while a system with larger value of κ indicates that it is ill-conditioned. A built-in-function matlab command $cond(...)$ is used for this purpose. The benchmark problems having scattered interior points are taken from Halton set that utilizes the following matlab coomands R = $haltonset$(Dim), craetes halton set on dimension Dim,
O = $scramble$(R,'RR2'), give duplicate set and RR2 is a scramble type,
X = net(O,M), generates $M \times Dim$ matrix contain the first M points in dimensions Dim from

Preprints (www.preprints.org) | NOT PEER-REVIEWED | Posted: 30 September 2020 doi:10.20944/preprints202009.0751.v1

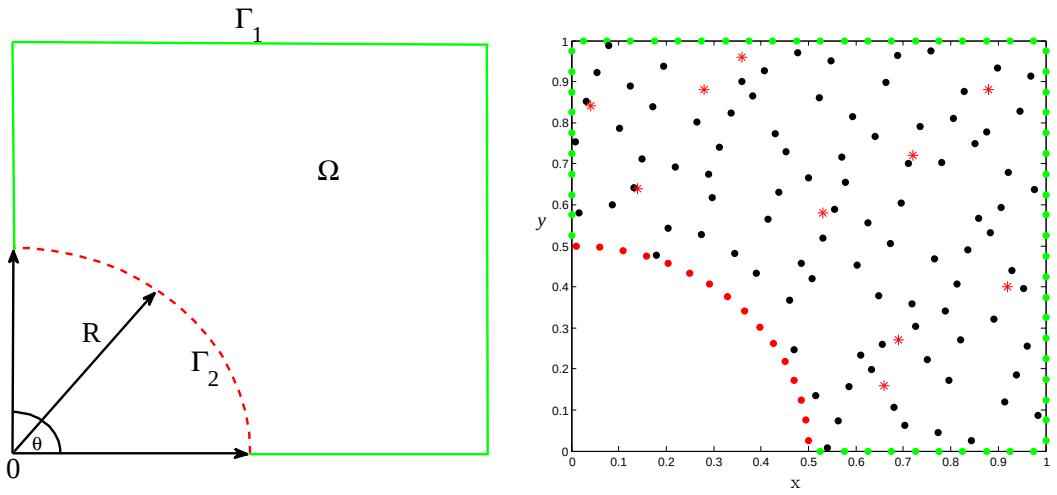

Figure 1: Model domain for test problem (1).

the point set O.

Test Problem 1. The partial differential equation is given in (1) with constant coefficients $k_{1,1}(\hat{\mathbf{v}}) = -1$, $k_{1,2}(\hat{\mathbf{v}}) = 0$ and $k_{2,2}(\hat{\mathbf{v}}) = -1$ reduces to Poisson equation and studied in Ref. [27] with the same nonlocal multipoint boundary condition. We consider the same problem with the same analytical solution

$$u(\hat{\mathbf{v}}) = x \exp(y^2 - 1). \tag{18}$$

The domain is a unit rectangle having a cut of the radius $R = 0.5$, which is depicted in Fig. 1 (left). The functions f, g and h are calculated according to the exact solution (18).

The representation of the solution domain and distribution of the nodes are depicted in Fig. 1. In Fig. 1 (right), the distinct scattered points marked with black dot represent an interior portion of the solution domain. The regularly distributed points marked with red dot represent the boundary part Γ_2 and the regularly distributed points marked with green dot represent the boundary part Γ_1. The scattered points marked with red asterisk are the points of the set $\Omega^\star$.

In case of Test Problem (1), the effect of the shape parameters (ϵ or ϵ_o), the parameter γ and the nodes are shown in Figs. 2 and 3 on the proposed methods using IMQ6 and MQ RBF as basis functions. From these figures, we can see that the methods based on IMQ6 RBF are better in accuracy and conditioning as compared to the methods based on MQ RBF. However, when the shape parameter is large, κ of the methods based on MQ RBF is small but the accuracy of the methods is low. The methods RCM1 and RCM2 also give quite good results for some value of ϵ_o (see Fig. 3). The proposed methods IRCM1 and IRCM2 give reasonable accuracy for a wide range of ϵ (see Fig. 2). Figure 3 (right) shows that the RCM2 is accurate than the RCM1 for dense grid and $\epsilon_o = 2$. However, κ of RCM2 is worse than RCM1.

Fig. 2 indicates that the IRCM1 is slightly good in conditioning than IRCM2. However, IRCM2 are much better in accuracy for a small value of ϵ. When the value of ϵ increases the error norms of the methods come close to each other (see Fig 2 (left)). The conditioning of both methods IRCM1 and IRCM2 are going to become better, up to certain limit when the value of ϵ increases. After this limit, it does not much affect the κ of the coefficient matrix. The behavior

Preprints (www.preprints.org) | NOT PEER-REVIEWED | Posted: 30 September 2020 doi:10.20944/preprints202009.0751.v1

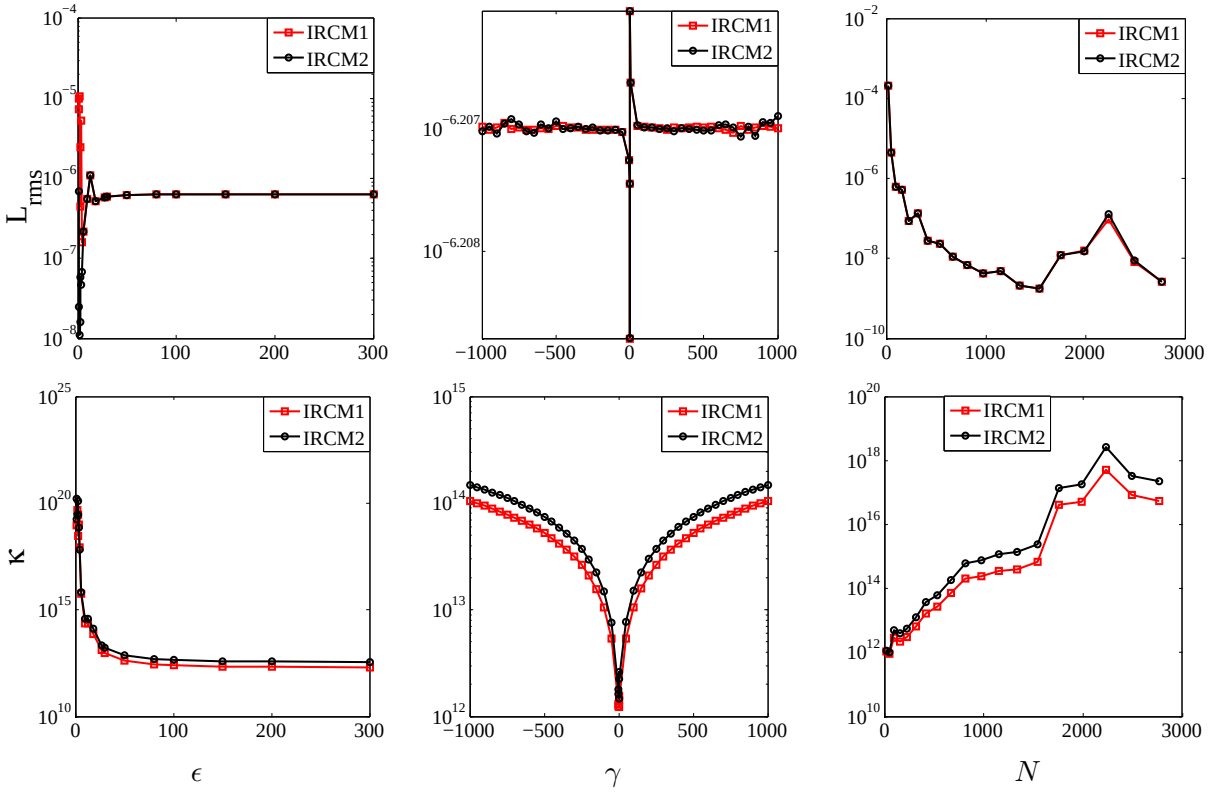

Figure 2: Test Problem 1, Accuracy and κ versus ϵ, γ and N: $\hat{\Gamma}_1 = 60$, $\hat{\Gamma}_2 = 16$, $\gamma = 1$, $\epsilon = 80$ and $N = 94$ when its influence is interestless.

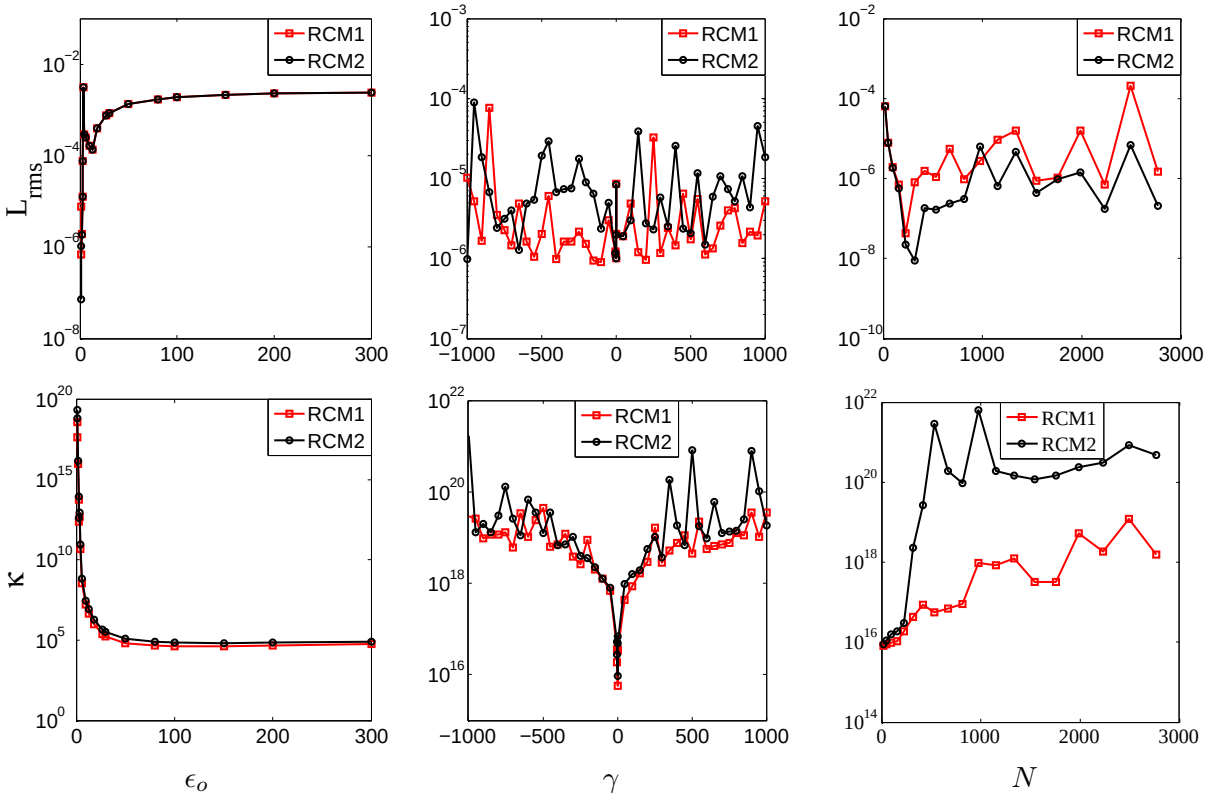

Figure 3: Test Problem 1, Accuracy and κ versus ϵ_o, γ and N: $\hat{\Gamma}_1 = 60$, $\hat{\Gamma}_2 = 16$, $\gamma = 1$, $\epsilon_o = 2$ and $N = 94$ when its influence is interestless.

Preprints (www.preprints.org) | NOT PEER-REVIEWED | Posted: 30 September 2020 doi:10.20944/preprints202009.0751.v1

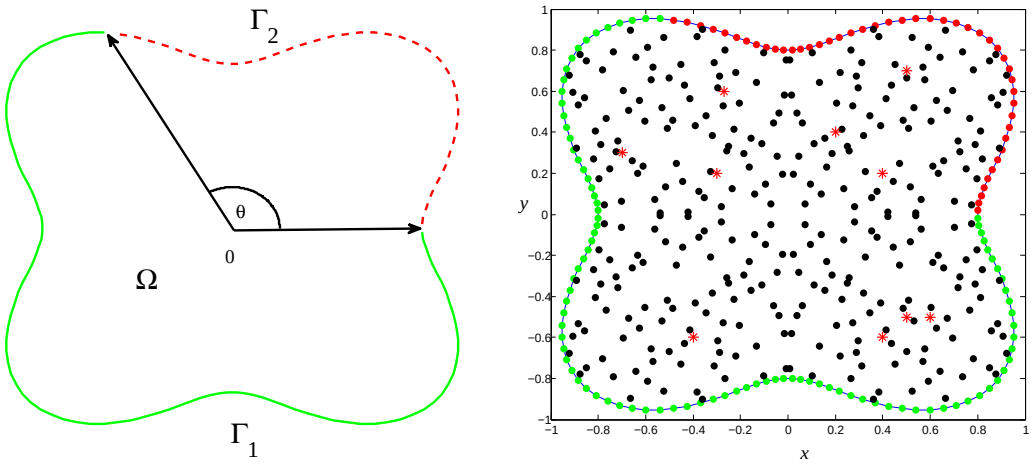

Figure 4: Model domain for test problem (2).

of IMQ6 RBF is same as the MQ RBF which give quite good results for a small value of shape parameter along with high κ of the coefficient matrix. Figures 2 (left) and 3 (left) also indicate that accuracy of the IRCM1 and IRCM2 is better for a very wide range of the value of ϵ as compared to the RCM1 and RCM2.

The effect of the collocation nodes on the accuracy of the proposed methods based on IMQ6 basis is also investigated. The value of the shape parameter is considered $\epsilon = 80$. The methods IRCM1 and IRCM2 give quite good results. As the nodal points increase, we see good agreement between solutions of IRCM1 and IRCM2 with exact one. However, κ increases for dense nodes while keeping the fixed value of the shape parameter $\epsilon = 80$.

The NBC (3) is defined comparatively on a small part of the boundary. But from Figs. 2 and 3 (middle), we see that the NBC has a quite strong negative influence on the κ of the coefficient matrices correspond to the methods RCM1, RCM2, IRCM1, and IRCM2. However, this influence is weak in case of IRCM1 and IRCM2 as compare to the methods RCM1 and RCM2. From Fig. 2 (middle), we can observe that both the methods IRCM1 and IRCM2 give same lowest and highest value of error norm. The highest and lowest error norms are $6.222e^{-7}$ and $6.184e^{-7}$ corresponding to $\gamma = 2$ and $\gamma = 0$. The influence of the NBC (3) is also weak on the κ of the coefficient matrices correspond to the methods IRCM1 and IRCM2 as compared to the methods RCM1 and RCM2. When $\epsilon_o = 2$ and $\epsilon = 80$, the methods RCM1 and RCM2 are most poorly ill-conditioned either the absolute value of γ increases as compared to the methods IRCM1 and IRCM2.

Test Problem 2. Consider the equation given in (1) with variables coefficients $k_{1,1}(\hat{\mathbf{v}}) = 5(1 + x^2 + y^2)$, $k_{1,2}(\hat{\mathbf{v}}) = 1 + \frac{xy}{2}$ and $k_{2,2}(\hat{\mathbf{v}}) = 3(1 + x^2 + y^2)$. The functions f, g and h are chosen such that the exact solution gets the form [1]:

$$u(\hat{\mathbf{v}}) = \cos(y)\exp(x - y).$$

Here in this example, we have considered an irregular-shaped domain defined by

$$x = p(\theta)\cos(\theta), \quad y = p(\theta)\sin(\theta), \quad p(\theta) = \frac{5 - \cos(4\theta)}{5}, \quad 0 \leq \theta \leq 2\pi, \tag{19}$$

where $p(\theta)$ is the radius of the domain which depends on the polar angle θ.

Preprints (www.preprints.org) | NOT PEER-REVIEWED | Posted: 30 September 2020 doi:10.20944/preprints202009.0751.v1

The representation of the domain for Test Problem (2) is depicted in Fig. 4. In Fig. 4 (left), the boundary parts Γ_2 $(0 \leq \theta \leq 2\pi/3)$ and Γ_1 $(2\pi/3 < \theta < 2\pi)$ are represented by red dashed and green solid lines respectively.

The influence of shape parameters, the parameter γ and nodal points on the accuracy and conditioning of the methods are shown in Figs. 5 and 6. The accuracy of IRCM2 is good as compared to the method IRCM1 for different values of shape parameter ϵ as shown in Fig. 5 (left). Although, both the methods are most poorly ill-conditioned for a small value of shape parameter ϵ while the method IRCM2 give high accuracy for a small value of ϵ than IRMC1. It can be observed from these figures that the accuracy of the methods and κ of the coefficient matrices for a fixed value of ϵ increases when the number of nodes increases. In contrast to the methods based on MQ RBF, the κ of the coefficient matrices of IRCM1 and IRCM2 is small. This is because of ϵ which is large and is equal to 80. The system matrices of the proposed methods are ill-conditioned for a small value of ϵ. In addition, the effect of the parameter γ on the methods IRCM1 and IRCM2 is also small. The method IRCM2 give slightly accurate results for all values of γ, even though the κ of the coefficient matrix of IRCM1 is high for some values of γ as compared to the method IRCM2 (see Fig. 5 (middle)).

For dense nodes, the RCM2 give quite good results for $\epsilon_o = 2$ as compared to RCM1 as shown in Fig. 6. However, the results obtained from IRCM1 or IRCM2 and the conditioning of the methods are much better there. Again in this example, the NBC (3) has a strong negative influence on the conditioning of the methods based on MQ RBF. From Fig. 6, we see fluctuation in κ of the coefficient matrices associated with the methods RCM1 and RCM2 as well as in error norms as the value of γ changes. This fluctuation in error norms occur due to the small value of ϵ_o.

Test Problem 3. Reconsider the differential equation given in (1) with constant coefficients $k_{1,1}(\hat{\mathbf{v}}) = 3$, $k_{1,2}(\hat{\mathbf{v}}) = 1.5$ and $k_{2,2}(\hat{\mathbf{v}}) = 2$. The functions f, g and h are chosen such that the exact solution gets the form [1]

$$u(\hat{\mathbf{v}}) = \sin\left(\frac{x}{\sqrt{2}}\right)\cosh\left(\frac{2\sqrt{30}}{15}x - \frac{\sqrt{30}}{10}y\right).$$

The representation of the domain for Test Problem (3) is depicted in Fig. 7. The curve $\Gamma_2 \cup \Gamma_1$ is called Cassini curve and is defined by parametric equation: [1]

$$x = \frac{4}{5}p(\theta)\cos(\theta) - \frac{1}{5}, \quad y = \frac{4}{5}p(\theta)\sin(\theta), \quad p(\theta) = \left(\cos(3\theta) + \sqrt{2 - \sin^2(3\theta)}\right)^{1/3}, \quad 0 \leq \theta \leq 2\pi, \tag{20}$$

and rest of the terms give same meaning as defined in Test Problem (2). We consider Neumann boundary condition on the boundary part Γ_1. The normal component of the heat flux on the boundary is of the form:

$$-\left(k_{1,1}(\hat{\mathbf{v}})\frac{\partial}{\partial x}u(\hat{\mathbf{v}}) + k_{1,2}(\hat{\mathbf{v}})\frac{\partial}{\partial y}u(\hat{\mathbf{v}})\right)n_x - \left(k_{1,2}(\hat{\mathbf{v}})\frac{\partial}{\partial x}u + k_{2,2}\frac{\partial}{\partial y}u(\hat{\mathbf{v}})\right)n_y = q(\hat{\mathbf{v}}), \tag{21}$$

where $q(\hat{\mathbf{v}})$ is some given function. n_x and n_y are the components of unit outward normal vectors.

Preprints (www.preprints.org) | NOT PEER-REVIEWED | Posted: 30 September 2020 doi:10.20944/preprints202009.0751.v1

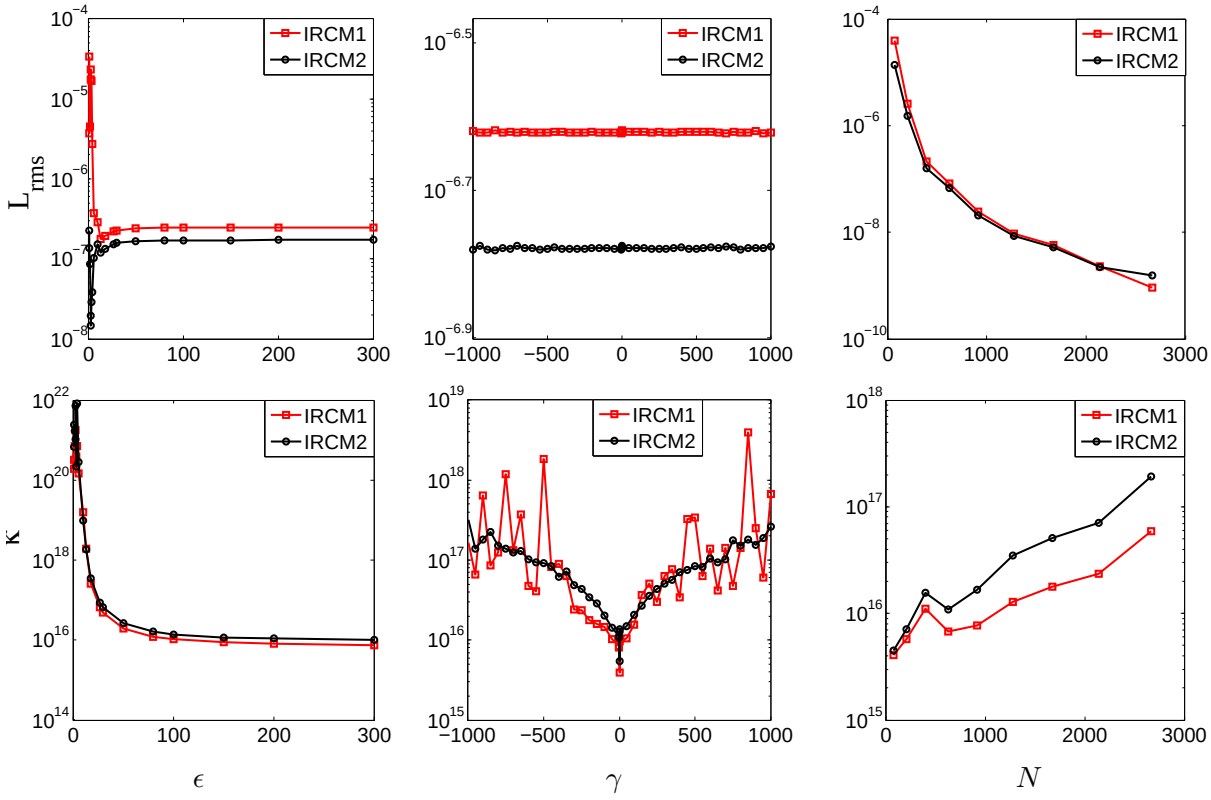

Figure 5: Test Problem 2, Accuracy and κ versus ϵ, γ and N: $\hat{\Gamma}_1 = 94$, $\hat{\Gamma}_2 = 46$, $\gamma = 1$, $\epsilon = 80$ and $N = 320$ when its influence is interestless.

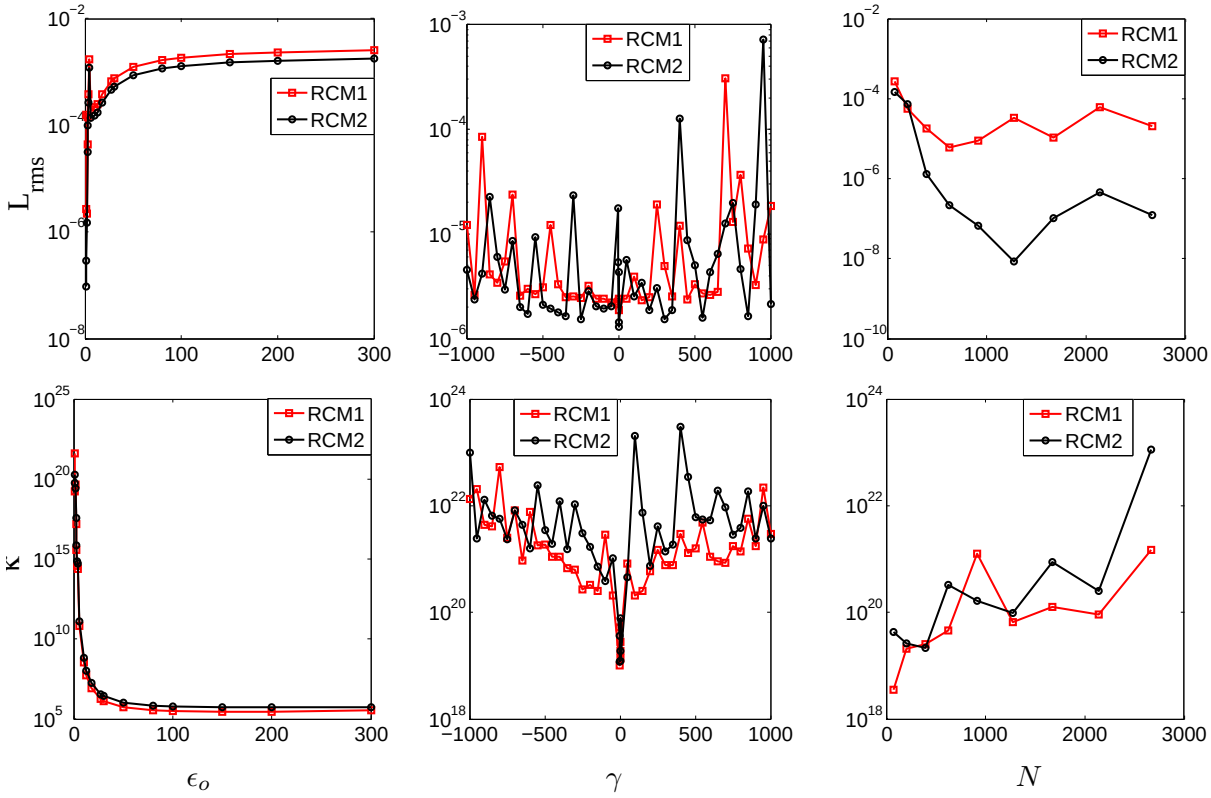

Figure 6: Test Problem 2, Accuracy and κ versus ϵ_o, γ and N: $\hat{\Gamma}_1 = 94$, $\hat{\Gamma}_2 = 46$, $\gamma = 1$, $\epsilon_o = 2$ and $N = 320$ when its influence is interestless.

Preprints (www.preprints.org) | NOT PEER-REVIEWED | Posted: 30 September 2020 doi:10.20944/preprints202009.0751.v1

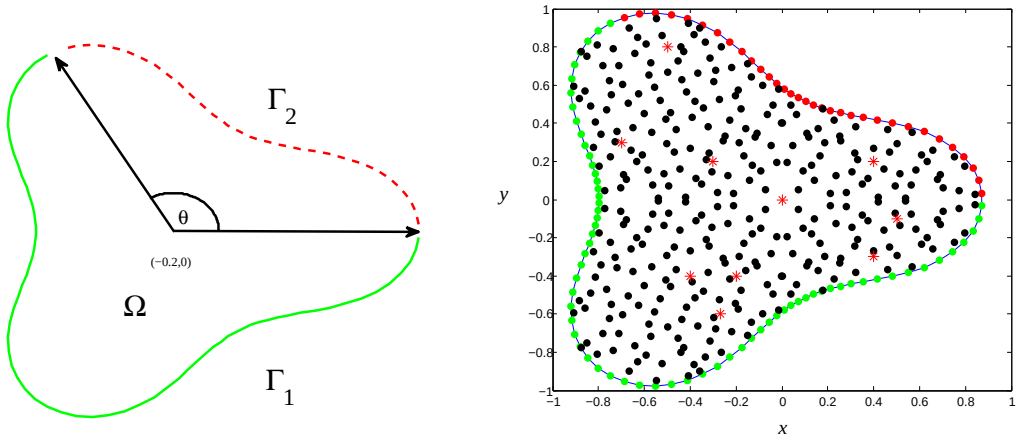

Figure 7: model domain for test problem (3).

Since it was shown in the paper [1] that RBFs approximation of the mixed connected boundary conditions, i.e., Dirichlet boundary condition is specified on some part of the boundary and Neumann condition is defined on the rest of boundary, is too much low in accuracy. If we specified Neumann boundary condition on boundary part Γ_1, then the accuracy of the boundary condition will be too low. Since, we use RBFs approximation (i.e., using MQ or IMQ6 RBF) to approximate the mixed connected boundary condition, i.e., the multi-point and Neumann boundary condition, and the solution inside the domain. So, obviously, it will also affect the approximate solution inside the solution domain. To avoid this problem, we used the same procedure as it is done above for Dirichlet boundary condition but replaced the system of equation obtained from boundary part Γ_1 with

$$
\begin{aligned}
&-\sum_{k=1}^{M}\beta_k\{\left(k_{1,1}(\hat{\mathbf{v}})\frac{\partial}{\partial x}\phi_k(\hat{\mathbf{v}})+k_{1,2}(\hat{\mathbf{v}})\frac{\partial}{\partial y}\phi_k(\hat{\mathbf{v}})\right)n_x+\left(k_{1,2}(\hat{\mathbf{v}})\frac{\partial}{\partial x}\phi_k+k_{2,2}\frac{\partial}{\partial y}\phi_k(\hat{\mathbf{v}})\right)n_y\}-\\
&\sum_{i=1}^{N}\lambda_i\{\left(k_{1,1}(\hat{\mathbf{v}})\frac{\partial}{\partial x}(\phi_i(\hat{\mathbf{v}})+\omega_i(\hat{\mathbf{v}}))+k_{1,2}(\hat{\mathbf{v}})\frac{\partial}{\partial y}(\phi_i(\hat{\mathbf{v}})+\omega_i(\hat{\mathbf{v}}))\right)n_x+\\
&\left(k_{1,2}(\hat{\mathbf{v}})\frac{\partial}{\partial x}(\phi_i(\hat{\mathbf{v}})+\omega_i(\hat{\mathbf{v}}))+k_{2,2}\frac{\partial}{\partial y}(\phi_i(\hat{\mathbf{v}})+\omega_i(\hat{\mathbf{v}}))\right)n_y\}=q(\hat{\mathbf{v}}),\qquad \hat{\mathbf{v}}\in\hat{\Gamma}_1.
\end{aligned}
\tag{22}
$$

The influence of shape parameters (ϵ or ϵ_o), the parameter γ and the number of nodes for Test problem (3) are shown in Figs. 8 and 9. It can be seen from Figs. 8 and 9, (right) that the proposed methods give good accuracy for dense grid whether RBF basis are MQ or IMQ6. But the κ of the coefficient matrices associated with the methods RCM1 and RCM2 are high. From Fig. 8 (top middle), we see that when $\gamma = 0$ the error norms of the methods IRCM1 and IRCM2 are $1.175e^{-6}$ and $1.226e^{-6}$ respectively.

Now we check the influence of the parameter γ on the methods IRCM1 and IRCM2 when the shape parameter is small. The value of the shape parameter $\epsilon = 2$ is taken for each problem. We see from Fig. 11 that IRCM2 give quite a good accuracy for a small value of shape parameter in

Preprints (www.preprints.org) | NOT PEER-REVIEWED | Posted: 30 September 2020 doi:10.20944/preprints202009.0751.v1

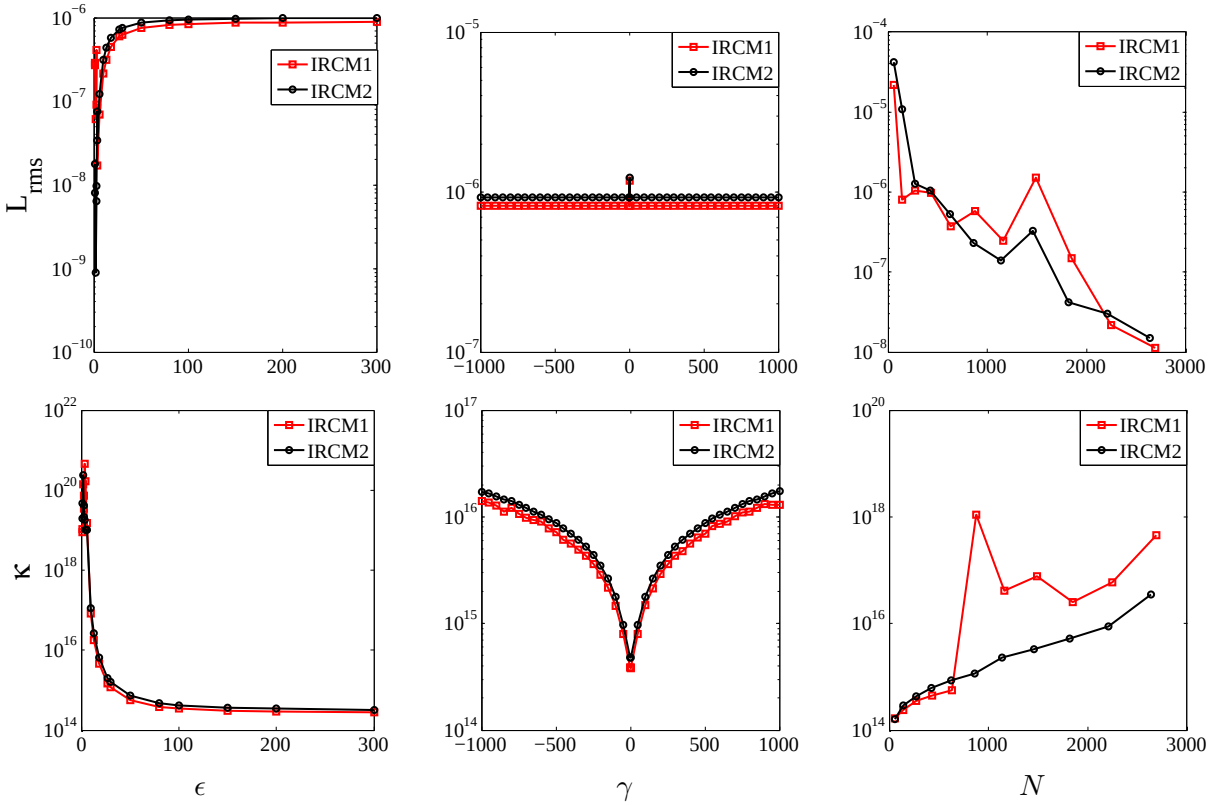

Figure 8: Test Problem 3, Accuracy and κ versus ϵ, γ and N: $\hat{\Gamma}_1 = 67$, $\hat{\Gamma}_2 = 33$, $\gamma = 1$, $\epsilon_o = 2$, $\epsilon = 80$ and $N = 312$ when its influence is interestless.

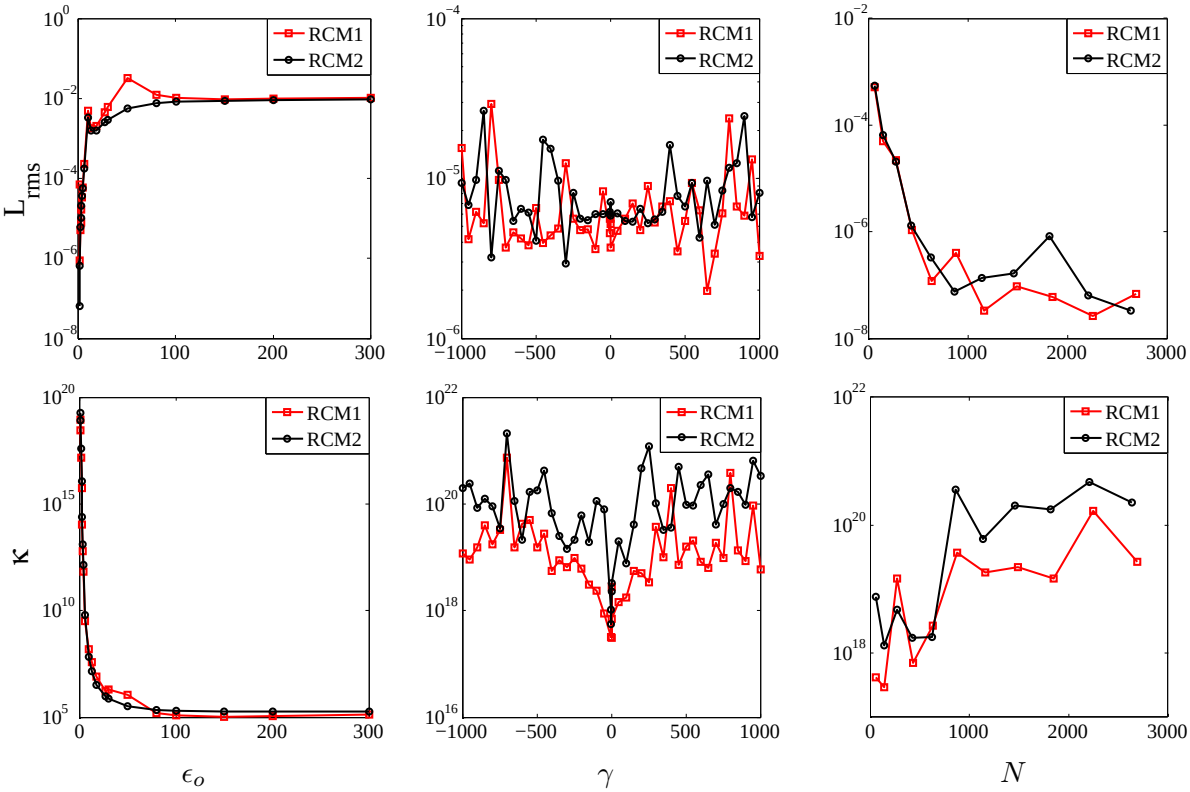

Figure 9: Test Problem 3, Accuracy and κ versus ϵ_o, γ and N: $\hat{\Gamma}_1 = 67$, $\hat{\Gamma}_2 = 33$, $\gamma = 1$, $\epsilon_o = 2$ and $N = 312$ when its influence is interestless.

Preprints (www.preprints.org) | NOT PEER-REVIEWED | Posted: 30 September 2020 doi:10.20944/preprints202009.0751.v1

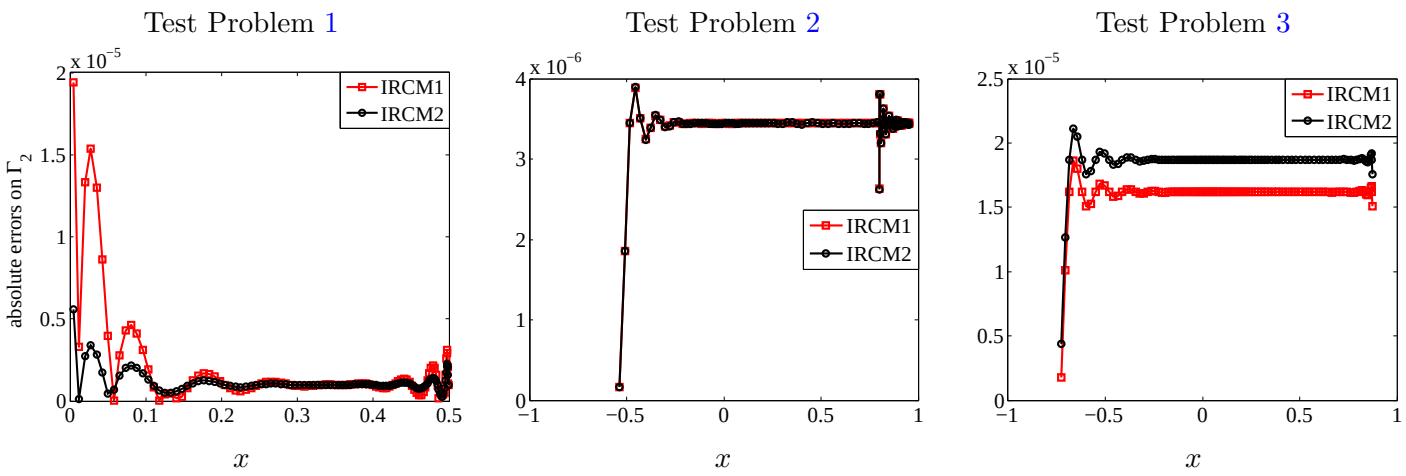

Figure 10: Test Problem 1-3, The absolute errors $|\mathbf{u}(\hat{\mathbf{v}}) - u(\hat{\mathbf{v}})|$ using the methods IRCM1 and IRCM2 versus x on boundary part Γ_2. $\epsilon = 80$ and $\gamma = 1$.

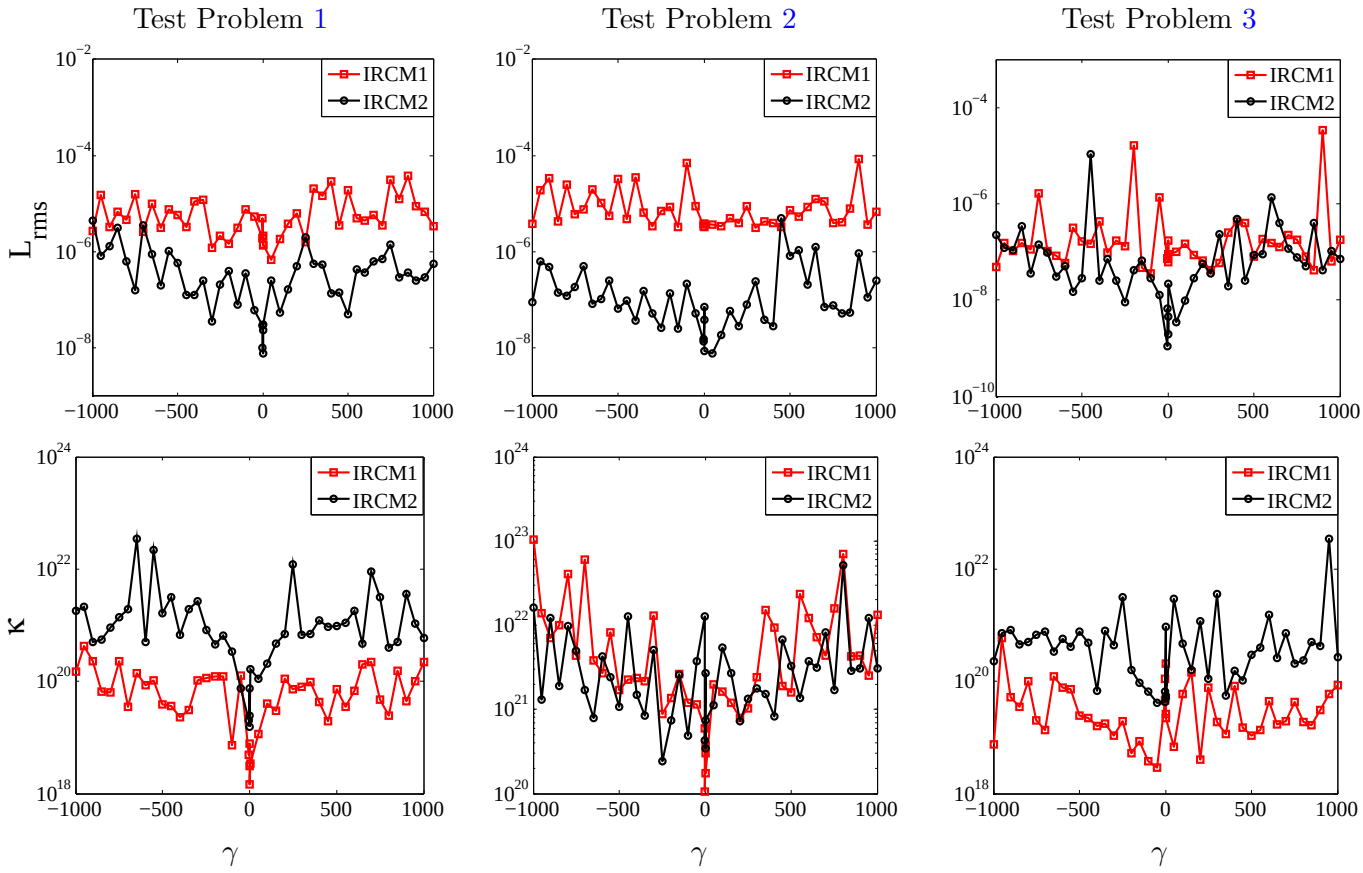

Figure 11: Test Problem 1-3, Accuracy and κ versus γ. $\epsilon = 2$.

Preprints (www.preprints.org) | NOT PEER-REVIEWED | Posted: 30 September 2020 doi:10.20944/preprints202009.0751.v1

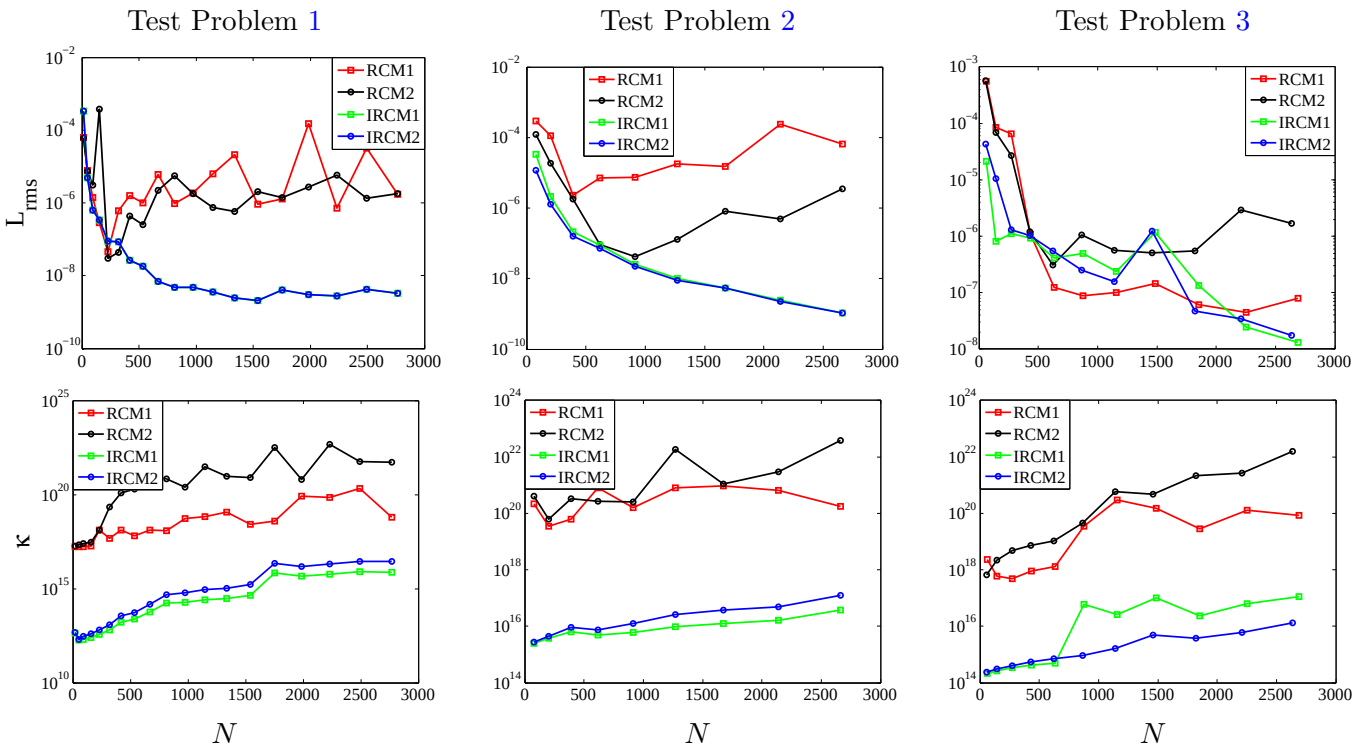

Figure 12: Test Problem 1-3, Accuracy and κ versus N. $\epsilon = 150$, $\epsilon_o = 2$ and $\gamma = 20$.

all Test Problems 1-3. The accuracy is good when the value of γ is zero or near to zero. It can be observed from this figure that the κ and the accuracy of the proposed methods deteriorate when the absolute value of γ increases. In contrast, when the value of shape parameter is high (i.e., $\epsilon = 80$) the κ deteriorates but the accuracy does not affect much when $|\gamma|$ is increased (see middle of Figs. 2, 5 and 8). The absolute error of IRCM1 and IRCM2 of the unknown solution on the boundary part Γ_2 is shown in Fig. 10. From this figure, we observed that both the methods IRCM1 and IRCM2 give quite a good accuracy.

Accuracy in term of error norm and conditioning of the coefficient matrices correspond to the proposed methods are shown in Fig. 12. The value of the parameters are $\epsilon = 150$, $\epsilon_o = 2$ and $\gamma = 20$. We observed from this figure that the proposed methods based on integrated MQ RBF perform well both in terms of accuracy and conditioning. We have also seen that different types of boundary conditions (i.e. Dirichlet and Neumann conditions) do not much affect the conditioning and accuracy of the proposed methods IRCM1 and IRCM2.

5 Conclusion

A collocation method based on MQ and IMQ6 is set up for the numerical solution of elliptic boundary value problem with variable coefficients involving NMBC. The comparison is made between Kansa's approach and the method discussed in the paper [1]. This approach can be extended to a higher dimension without any effort. However, two-dimensional problems with Dirichlet and Neumann boundary condition was considered in the different domain for examination. Based on benchmark examples, we conclude:

• For large value of the shape parameter ϵ, we have seen better agreement of the numerical solution of IRCM1 and IRCM2 with the exact solution (see Figs. 2, 3, 5, 6, 8 and 9).

• For a wide range of shape parameter, the collocation method based on IMQ6 RBF give quite good results while on the other side a method based on MQ RBFs is very sensitive. Accurate results can be obtained from both the collocation methods based MQ and IMQ6 RBF for the optimal value of shape parameter which is still an open problem.

• The method based on IMQ6 RBF is well conditioned as compared to the collocation method based on MQ RBF (see Fig. 10) for large value of shape parameter ϵ. However, the methods IRCM1, IRCM2, RCM1 and RCM2 become most poorly ill-conditioned for small value of shape parameter ϵ (see Figs. 2, 3, 5, 6, 8 and 9).

• The methods IRCM1 and IRCM2 are less restrictive to the NMBC for large value of shape parameter as compared to a small value of shape parameter i.e., when the shape parameter is large then accuracy of the methods IRCM1 and IRCM2 are approximately same for all values of γ and κ increases when the absolute value of γ increases (see Figs. 2, 5 and 8). On the other side, for a small value of shape parameter the accuracy of the methods IRCM1 and IRCM2 also decreases (see Fig. 10).

• The method based on IMQ6 RBFs give quite good results for coarse and dense grid while κ is also better as compared to the methods RCM1 and RCM2 (see Fig. 10).

Author Contribution: Conceptualization, Supervision, Writing review and editing by Zaheer-ud-Din, Formal Analysis, Investigation, and Methodology by Masood Ahmad, Software, Data Curation, and Visualization by Muhammad Ahsan, Project administration by Abdel-Haleem Abdel-Aty, Funding acquisition by Emad E. Mahmood.

Acknowledgment: The authors are thankful for financial assistance of

1. Taif University Researchers Supporting Project Number (TURSP-2020/20), Saudi Arabia.
2. CECOS University, Peshawar.

References

[1] S. Reutskiy. A meshless radial basis function method for 2D steady-state heat conduction problems in anisotropic and inhomogeneous media. *Engineering Analysis with Boundary Elements*, 66:1–11, 2016.

[2] G. Fasshauer. *Meshfree approximation methods with matlab*, volume 6. World Scientific Publishing Co. Pte. Ltd.

[3] S. Sarra. Integrated multiquadric radial basis function approximation methods. *Computers and Mathematics with Application*, 51:1283–1296, 2006.

[4] R. Hardy. Multiquadratic equations for topography and other irregular surfaces. *Journal of Geophysical Research*, 76, 1971.

[5] R. Franke. Scattered data interpolation tests of some methods. *Mathematics of Computation*, 38, 1982.

[6] G. Fasshauer. Newton iteration with multiquadratics for the solution of nonlinear PDEs. *Computers and Mathematics with Applications*, 43:423–438, 2002.

[7] J. Wang and G. Liu. On the optimal shape parameters of radial basis functions used for 2-D meshless methods. *Computers Methods in Applied Mechanics and Egineering*, 191:2611–2630, 2002.

[8] L. Ballestra and G. Pacelli. Computing the survival probability density function in jump-diffusion models: a new approach based on radial basis functions. *Engineering Analysis with Boundary Elements*, 35:1075–1084, 2011.

[9] L. Ballestra and G. Pacelli. Pricing European and American options with two stochastic factors: A highly efficient radial basis function approach. *Journal of Economic Dynamics and Control*, 37:1142–1167, 2013.

[10] Siraj-ul-Islam, I. Aziz, and M. Ahmad. Numerical solution of two-dimensional elliptic PDEs with nonlocal boundary conditions. *Computers and Mathematics with Applications*, 69:180–205, 2015.

[11] L. Luh. The shape parameter in the Gaussian function. *Computers and Mathematics with Applications*, 63:453–461, 2012.

[12] O. Davydov and D. Oanh. On the optimal shape parameter for Gaussian radial basis function finite difference approximation of the Poisson equation. *Computers and Mathematics with Applications*, 62:27–49, 2001.

[13] A. Cheng. Multiquadric and its shape parameter - a numerical investigation of error estimate, condition number, and round-off error by arbitrary precision computation. *Engineering Analysis with Boundary Elements*, 36:220–239, 2012.

[14] C. Huang, H. Yen, and A. Cheng. On the increasingly flat radial basis function and optimal shape parameter for the solution of elliptic PDEs. *Engineering Analysis with Boundary Elements*, 34:802–809, 2010.

[15] M. Scheuerer. An alternative procedure for selecting a good value for the parameter c in RBF-interpolation. *Advances in Computational Mathematics*, 34:105–126, 2011.

[16] M. Uddin. On the selection of a good value of shape parameter in solving time-dependent partial differential equations using RBF approximation method. *Applied Mathematical Modelling*, 38:135–144, 2014.

[17] M. Esmaeilbeigi and M. Hosseini. A new approach based on the genetic algorithm for finding a good shape parameter in solving partial differential equations by Kansa's method. *Applied Mathematics and Computation*, 249:419–428, 2014.

[18] S. Kazem and F. Hadinejad. Promethee technique to select the best radial basis functions for solving the 2-dimensional heat equations based on hermite interpolation. *Engineering Analysis with Boundary Elements*, 50:29–38, 2015.

[19] A. Golbabi, E. Mohebianfar, and H. Rabiei. On the new variable shape parameter strategies for radial basis functions. *Computational and Applied Mathematics*, 34:691–704, 2015.

[20] M. Kadalbajoo, A. Kumar, and L. Tripathi. A radial basis functions based finite differences method for wave equation with an integral condition. *Applied Mathematics and Computation*, 238:8–16, 2015.

[21] L. Yan and F. Yang. The method of approximate particular solutions for the time-fractional diffusion equation with non-local boundary condition. *Computers and Mathematics with Applications*, 70:2716–2732, 2015.

[22] M. Dehghan and M. Tatari. On the solution of the non-local parabolic partial differential equations via radial basis functions. *Applied Mathematical Modelling*, 52:461–477, 2009.

[23] M. Dehghan and A. Shokri. A meshless method for numerical solution of the one-dimensional wave equation with an integral conditions using radial basis functions. *Numerical Algorithms*, 52:461–477, 2009.

[24] S. Kazem and J. Rad. Radial basis functions method for solving of a non-local boundary value problem with neumann's boundary conditions. *Applied Mathematical Modelling*, 36:2360–2369, 2012.

[25] S. Sajavicius. Optimization, conditioning and accuracy of radial basis function method for partial differential equations with nonlocal boundary conditions a case of two-dimensional poisson equation. *Engineering Analysis with Boundary Elements*, 37:788–804, 2013.

[26] S. Sajavicius. Radial basis function method for a multidimensional linear elliptic equation with nonlocal boundary conditions. *Computers and Mathematics with Applications*, 87:1407–1420, 2014.

[27] S. Sajavicius. Radial basis function collocation method for an elliptic problem with nonlocal multipoint boundary condition. *Engineering Analysis with Boundary Elements*, 67:164–172, 2016.

[28] L. Ling and M. Trummer. Multiquadric collocation method with integral formulation for boundary layer problems. *Computers and Mathematics with Applications*, 48:927–941, 2004.

[29] N. Mai-Duy and T. Tran-Cong. A multidomain integrated radial basis function collocation method for elliptic problems. *Applied Mathematical Modelling*, 27:197–220, 2003.

[30] N. Mai-Duy and T. Tran-Cong. Solving high order ordinary dierential equations with radial basis function networks. *International Journal of Numerical Methods in Engineering*, 62:824–852, 2005.

[31] N. Mai-Duy and T. Tran-Cong. Solving high order partial dierential equations with indirect radial basis function networks. *International Journal of Numerical Methods in Engineering*, 63:1636–1654, 2006.

[32] E. Kansa, H. Power, G. Fasshauer, and L. Ling. A volumetric integral radial basis function method for time- dependent partial dierential equation: I. formulation. *Engineering Analysis with Boundary Elements*, 28:1191–1206, 2004.

[33] N. Mai-Duy and T. Tran-Cong. An integrated-RBF technique based on Garlerkin formulation for elliptic differential equations. *Engineering Analysis with Boundary Elements*, 33:191–199, 2009.

[34] N. Thai-Quang, K. Le-Cao, N. Mai-Duy, C. Tran, and T. Tran-Cong. A numerical scheme based on compact integrated RBFs and Adams- Bashforth/CrankNicolson algorithms for diffusion and unsteady fluid flow problems. *Engineering Analysis with Boundary Elements*, 37:1653–1667, 2013.